

See discussions, stats, and author profiles for this publication at: <https://www.researchgate.net/publication/263959257>

# Charcoal Ash as an Adsorbent for Ni(II) Adsorption and Its Application for Wastewater Treatment

ARTICLE in JOURNAL OF CHEMICAL & ENGINEERING DATA · JANUARY 2012

Impact Factor: 2.04 · DOI: 10.1021/je200953h

CITATIONS

15

READS

110

5 AUTHORS, INCLUDING:



Reza Katal

22 PUBLICATIONS 248 CITATIONS

SEE PROFILE



M. Sharifzadeh

Islamic Azad University - Science and Research...

32 PUBLICATIONS 354 CITATIONS

SEE PROFILE



Mohammad Ali Ghayem

Iran University of Science and Technology

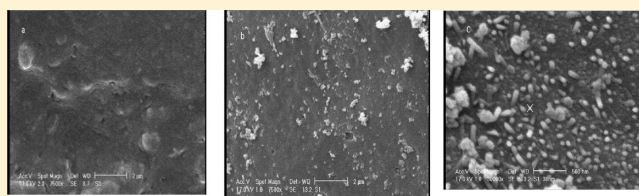
8 PUBLICATIONS 25 CITATIONS

SEE PROFILE

## Charcoal Ash as an Adsorbent for Ni(II) Adsorption and Its Application for Wastewater Treatment

Reza Katal,<sup>†</sup> Ehsan Hasani,<sup>‡</sup> Maysam Farnam,<sup>‡</sup> Mazyar Sharifzadeh Baei,<sup>\*,§</sup> and Mohammad Ali Ghayyem<sup>||</sup><sup>†</sup>Faculty of Chemical Engineering, Tarbiat Modares University, Tehran, Iran<sup>‡</sup>Department of Engineering, Shahrood Branch, Islamic Azad University, Shahrood, Iran<sup>§</sup>Department of Chemical Engineering, Islamic Azad University, Ayatollah Amoli Branch, Amol, Iran<sup>||</sup>Petroleum University of Technology, Ahwaz, Iran

**ABSTRACT:** The aim of present research is to investigate sorption characteristic of nanoadsorbent charcoal ash (ash) for the removal of Ni(II) from aqueous solutions and wastewater. The sorption of Ni(II) is carried out by batch method. The optimum conditions of sorption were found to be as follows: a sorbent amount of 3 g in 100 mL of aqueous solutions, contact time of 120 min, and pH 4. In optimum conditions, removal efficiency was 94.2 % for the Ni(II). Three equations, i.e., Morris–Weber, Lagergren, and pseudo second order, have been tested to track the kinetics of the removal process. The Langmuir, Freundlich, and D-R are subjected to sorption data to estimate sorption capacity. It can be concluded that ash has the potential to remove Ni(II) ions from aqueous solutions at different concentrations. Desorption efficiency had been tested by water saturated with CO<sub>2</sub> and by aqueous solution of NaOH, and the results were not considerable. The effect of temperature has been studied; it was found that increasing temperature has a positive effect on the adsorption, and the thermodynamic parameters  $\Delta H$ ,  $\Delta S$ , and  $\Delta G$  are evaluated. Thermodynamic parameters showed that the adsorption of Ni(II) onto ash was feasible, spontaneous, and endothermic under the studied conditions. At the end, ash was used for plating wastewater treatment so that the results were considerable. The removal efficiency of COD, Cr, Ni(II), Zn(II), and color were 68.3, 75.4, 91.5, 92.8, and 63.5 %, respectively. In this paper, different parameter such as pH, temperature, etc. were studied for Ni(II) adsorption onto ash, meanwhile this adsorbent is used for real wastewater (plating wastewater) treatment.



## ■ INTRODUCTION

Heavy metal ions have become an ecotoxicological hazard of prime interest and increasing significance, because of their accumulation in living organisms.<sup>1</sup> Ni(II) is present in effluents of a large number of industries. People often suffer from allergy due to exposure to nickel-containing materials, and the carcinogenic effects of nickel have also been well documented.<sup>2</sup> Nickel is a toxic heavy metal widely used in silver refineries, electroplating, zinc base casting, and storage battery industries.<sup>3</sup> Current treatment processes for Ni(II) removal from wastewater include precipitation, coagulation, ion exchange, membrane separation, lime softening, and adsorption. Compared with other methods, adsorption technology has received much more attention because it is convenient and economical for reducing trace quantities of heavy metals.<sup>4,5</sup> Though the use of commercial activated carbon is a well-known adsorbent for the removal of heavy metals from water and wastewater, the high cost of activated carbon limits its use as an adsorbent in developing countries. Hence, several research workers used different low-cost adsorbents such as coconut coir pith,<sup>6</sup> sawdust,<sup>7</sup> sludge ash,<sup>8</sup> banana pith,<sup>9</sup> activated phosphate rock,<sup>10</sup> vermiculite,<sup>11</sup> and montmorillonite.<sup>12</sup> In spite of several researchers adopting various low-cost adsorbents, there is still a need to develop

suitable adsorbents for the removal of heavy metal from aqueous solutions. Adsorption of trace heavy metals onto solid phases and associated surface coatings is considered very important in controlling heavy metal activity. In recent years considerable attention has been paid to the investigation of different types of low-cost sorbents especially using metal-oxide modified adsorbents, such as sand,<sup>13–15</sup> zeolite,<sup>16,17</sup> and diatomite.<sup>18</sup>

Fly ash is a waste material originating in great amounts in combustion processes. Although it may contain some hazardous substances, such as heavy metals, it is widely utilized in industry in many countries. For example, in 1994, approximately 6.74 million metric tons of coal fly ash was used in the United States in cement and concrete products.<sup>19</sup> Although fly ash utilization in construction and other civil engineering applications is expected to increase, it is unlikely that this will ever use all the fly ash generated. Research is therefore needed to develop new alternative environmental friendly applications that can further exploit fly ash. Potential environmental impacts of fly ash utilization have been extensively studied and are well

Received: September 2, 2011

Accepted: December 14, 2011

Published: January 6, 2012



understood. Leachability of heavy metals from ashes is relatively low<sup>20</sup> and thus the risks associated with the heavy metals liberation into the environment do not exceed an acceptable level. When used for acidity control in mining and sulfide ore treatment, the lignite fly ash reduced concentrations of dissolved metals in waters to values that meet the European regulatory limits for potable water.<sup>21</sup> Various kinds of ashes have been used as low-cost sorbents for the removal of heavy metals,<sup>20,22</sup> organics,<sup>23,24</sup> as well as dyes<sup>23,25–27</sup> from waters. The applicability of the fly ashes for water treatment depends strongly on their origin. Fly ashes from waste incinerators seem to be unsuitable because of their nonstable composition and properties. It was shown that both total contents of heavy metals as well as there leached (leached) amounts of these pollutants are higher in the case of the incinerator fly ashes in comparison with coal fly ashes.<sup>28</sup> Ash generated in sugar industry probably does not contain large amounts of toxic metals and has been widely used for adsorption of pollutants from waters.<sup>24,26</sup>

The present research was devoted to the application of ash for the removal of Ni(II) in batch mode. The effects of pH, temperature, contact time, and initial Ni(II) concentration were investigated. Isothermal models and kinetics of adsorption were studied, and thermodynamic parameters were determined. Also desorption efficiency had been tested by water saturated with CO<sub>2</sub> and by aqueous solution of NaOH. In the end, the adsorbent has been used for plating wastewater treatment.

## EXPERIMENTAL SECTION

**Ash Preparation and Characterizations.** For preparation of ash, charcoal was used; the procedure was putting it in an oven for 24 h after burning charcoal. For determining the initial composition of fly ash, 750 mg of dried ash sample was treated for 2 days with 20 mL of 200 g/L HF. Then 80 mL of 50 g/L H<sub>3</sub>BO<sub>3</sub> was added to dissolve a possible precipitate of CaF<sub>2</sub>. The determination of SiO<sub>2</sub> was performed according to the ASTM D 27956 molybdosilicate method and the SO<sub>3</sub> according to the ASTM D1757 gravimetric method. For all experiments, the measurements were carried out as triplicate runs. The physicochemical characterization of ash was performed using standard procedures. Characterization of the ash was carried out by surface area analysis, bulk density, particle size distribution analysis, and scanning electron microscopy (SEM). The surface area of the ash was measured by BET (Brunauer–Emmett–Teller nitrogen adsorption technique). The density of ash was determined by specific gravity bottle. The moisture content determination of adsorbent was carried out with a digital microprocessor-based moisture analyzer (Mettler-LP16). The particle size distribution analysis was carried out using a Particle Size Distribution analyzer (model 117.08, Malvern instruments, U.S.A.). The results of particle size distribution are shown in Table 1. To

**Table 1. Particle Size Distribution of the Ash (400–500 μm)**

adsorbent (μm)	ash (%)
400–420	24.2
420–440	23.4
440–460	27.1
460–480	20.3
480–500	10.2

understand the morphology of adsorption of Ni(II) on the ash, the samples were gold sputter coated and SEM micrographs were taken using SEM (model S3400, Hitachi, Japan). Table 2

**Table 2. Bulk Chemical Composition of Fly Ash**

oxide	g/kg
SiO <sub>2</sub>	247.9
Fe <sub>2</sub> O <sub>3</sub>	44.1
Al <sub>2</sub> O <sub>3</sub>	128.8
TiO <sub>2</sub>	2.4
CaO	483.8
MgO	42.6
SO <sub>3</sub>	44.3
Na <sub>2</sub> O	3.1
K <sub>2</sub> O	6.4

**Table 3. Characteristics of Ash**

adsorbent	ash
surface area (m <sup>2</sup> ·g <sup>-1</sup> )	62.1
bulk density (g·cm <sup>-3</sup> )	1.15
zero-point charge, pH	8
mean diameter (m)	2.4 × 10 <sup>-4</sup>

shows the chemical composition of ash. Bulk density and surface area are reported in Table 3. The zero-point charge of the ash was determined by the solid addition method.<sup>29</sup> The structure of ash was studied using X-ray diffractograms (XRDs) obtained from an X-ray diffractometer (model No. XRD 3000P, Seifert, Germany). Nickel concentrations in supernatants were analyzed by flame atomic absorption spectrophotometry, Perkin-Elmer model 2100 (Perkin-Elmer, Überlingen, Germany). The wavelength was 323 nm that allowed the measuring of Ni concentrations in the range 0–200 ppm without diluting the solutions. Flow rates were 3.03 min<sup>-1</sup> for air and 1.0 for acetylene.

**Preparation of Ni (II) Solutions.** A solution of Ni was prepared using analytical grade NiCl<sub>2</sub> provided by Merck Company and stored at room temperature. Before using of this powder, it was dried for 1 h at 120 °C.

**Batch Adsorption Experiments.** Adsorption experiments were carried out in 150 mL flasks, and the total volume of the reaction solution was kept at 100 mL. The flasks were shaken at 400 rpm for the required time in a water bath shaker. The effect of solution pH on the removal of ash was investigated over the pH range from 2 to 10. The initial solution pH was adjusted using 0.5 mol·L<sup>-1</sup> HCl or 0.5 mol·L<sup>-1</sup> NaOH. After equilibration, the suspension of the adsorbent was separated from solution by filtration using Whatman No. 42 filter paper. Blank experiments were conducted to ensure that no adsorption was taking place on the walls of the apparatus used. All experiments were conducted in duplicate and mean values were used. The results of these studies were used to obtain the optimum conditions for maximum heavy metal removal from aqueous solution. The experimental error was below 3%, the average data were reported. The removal efficiency of Ni(II), % removal, was calculated as

$$\% \text{ removal} = (C_i - C_f) / C_i \times 100 \quad (1)$$

where  $C_i$  is the initial concentration (mg·L<sup>-1</sup>) and  $C_f$  is the final concentration (mg·L<sup>-1</sup>).  $q$  is the amount of metal adsorbed per specific amount of adsorbent (mg/g). The sorption capacity at time  $t$ ,  $q_t$  (mg·g<sup>-1</sup>), was obtained as follows

$$q_t = (C_i - C_t) V / m \quad (2)$$

where  $C_i$  and  $C_t$  (mg·L<sup>-1</sup>) were the liquid-phase concentrations of solutes at initial and a given time  $t$ ,  $V$  was the solution volume, and



$m$  was the mass ash (g). The amount of adsorption at equilibrium,  $q_e$ , was given by

$$q_e = (C_i - C_e)V/m \quad (3)$$

where  $C_e$  ( $\text{mg}\cdot\text{L}^{-1}$ ) was the ion concentration at equilibrium.

**Desorption Experiments.** Leaching tests by water saturated with  $\text{CO}_2$  and aqueous solution of acetic acid were carried out. Exhaust ash samples, resulting from multielement sorption experiments, were used.

**Test by Water Saturated with  $\text{CO}_2$ .** Desorption experiments were carried out using pure water saturated with  $\text{CO}_2$  with an initial pH value of 9. A 3 g sample of exhaust ash was placed into 0.2 L of leaching solution. After shaking for 24 h at  $20^\circ\text{C}$ , the mixture was filtered by 0.45 mm Millipore filter and the eluate analyzed for metal ion concentration.

**Test by Aqueous Solution of NaOH.** These experiments were carried out using different concentration of NaOH aqueous solution. A 3 g sample of exhaust ash was placed into 0.2 L of leaching NaOH solution. The pH was adjusted to 9 during the experiments by small additions of NaOH aqueous solution. After shaking for 24 h at  $20^\circ\text{C}$ , the mixture was filtered by 0.45-mm Millipore filter; the metal ion content in the eluate was determined by atomic absorption.

## RESULTS AND DISCUSSION

**Surface Characterization.** The ash surface chemistry before and after adsorption were evaluated by SEM. The SEM with clear image with smooth shape in ash before adsorption was observed (Figure 1a). After adsorption (Figure 1b) light point is position of particles on the adsorbent after adsorption process. As can be seen in Figure 1c, the adsorbed particles were in the 30–60 nm range so this adsorbent has high potential in the nanometer size particle adsorption. EDX analysis of adsorbent before and after Ni(II) adsorption (data not shown) confirmed this observation. The presence of Ni(II) on ash proved that the Ni(II) removed from solution had been adsorbed onto ash.

The X-ray diffraction spectra can give information about the changes in the quantity of the amorphous parts in ash after adsorption. As could be seen from Figure 2 in the X-ray diffraction spectra of ash there were no peaks at  $2\theta$  about  $44^\circ$ – $53^\circ$  and  $77^\circ$  in Figure 2a but these peaks is appeared in the ash X-ray after adsorption process (Figure 2b) that associated nickel is adsorbed onto ash.<sup>30</sup>

**Effect of Contact Time.** The rate at which adsorption take place is of most important when designing batch adsorption experiments. Consequently, it is important to establish the time dependence of such systems under various process conditions. The experimental runs measuring the effect of contact time on the batch adsorption of metal solution containing 100 mg/L of Ni (II) at  $20^\circ\text{C}$  and initial pH value 4 and ash dose of 3 g in 100 mL is shown in Figure 3. For Ni(II), sorption rate reaches up to 94.2% when contact time is 120 min, and then little change of sorption rate is observed. This result revealed that adsorption of Ni(II) is fast and the equilibrium was achieved by 2 h of contact time. Taking into account these results, a contact time of 2 h was chosen for further experiments.

**Effect of pH Sorption.** The pH of the solution affects the charge on the surface of the adsorbents, so the change in pH also affects the adsorption process and the  $\text{H}^+$  ion concentration may react with the functional groups on the active sites on the adsorption surface. Figure 4 shows the zeta-potentials of the ash particles in water measured at various pH's. It can be seen

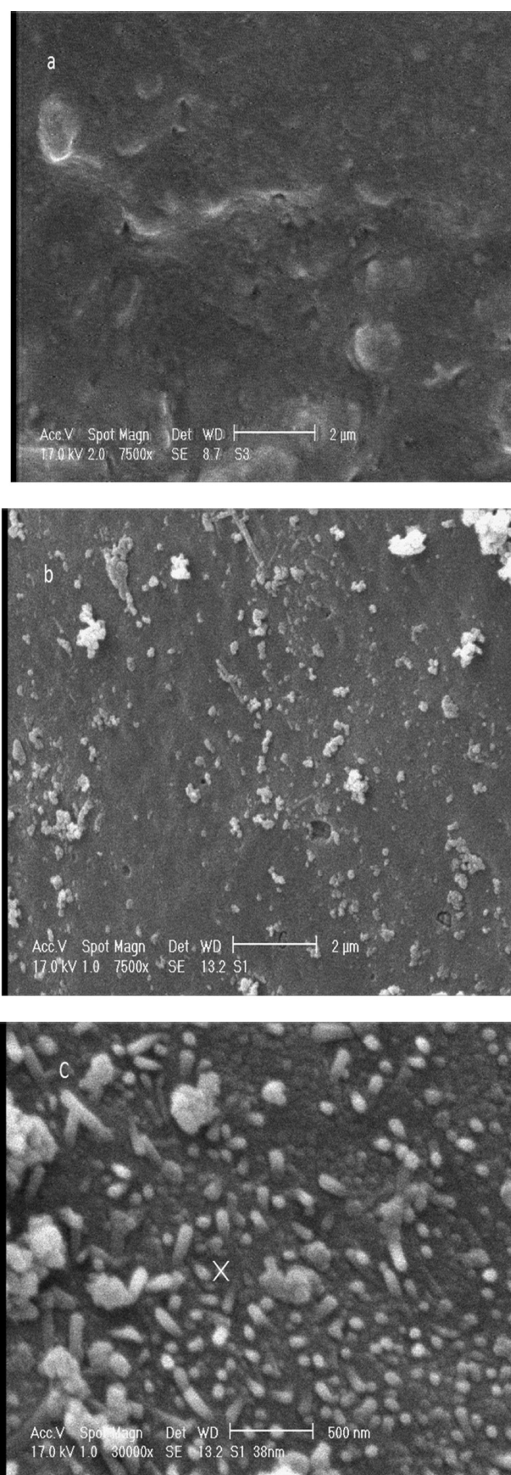


**Figure 1.** SEM image of ash before adsorption (a) after adsorption (b) and after adsorption with more zoom (c).

that the ash particles are negatively charged at low pH's and positively charged at high pH's, having a point of zero charge (PZC) at a pH of 8. Therefore, it can be expected that positively charged metal ions are likely to adsorb onto the negatively charged ash particles at a pH below 8. In general, adsorption of cations is favored at  $\text{pH} > \text{pH}_{\text{PZC}}$ . The pH of the solutions has been identified as the most important variable governing metal adsorption. This is partly due to the fact that hydrogen ions themselves are strong competing ions and partly

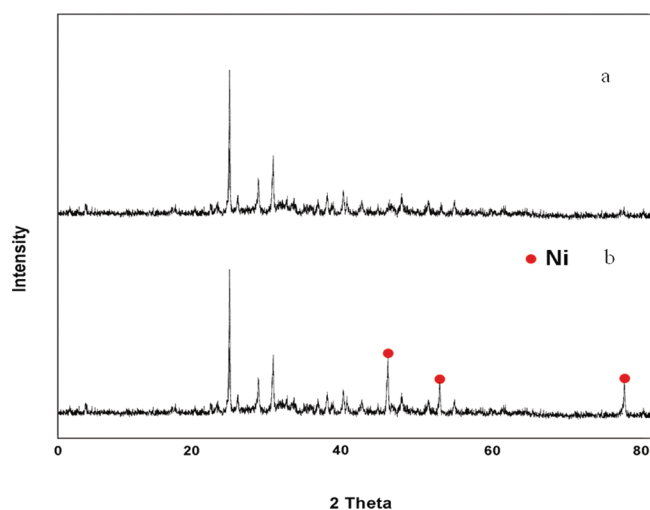


Figure 2. XRD pattern of ash (a) before and (b) after adsorption.

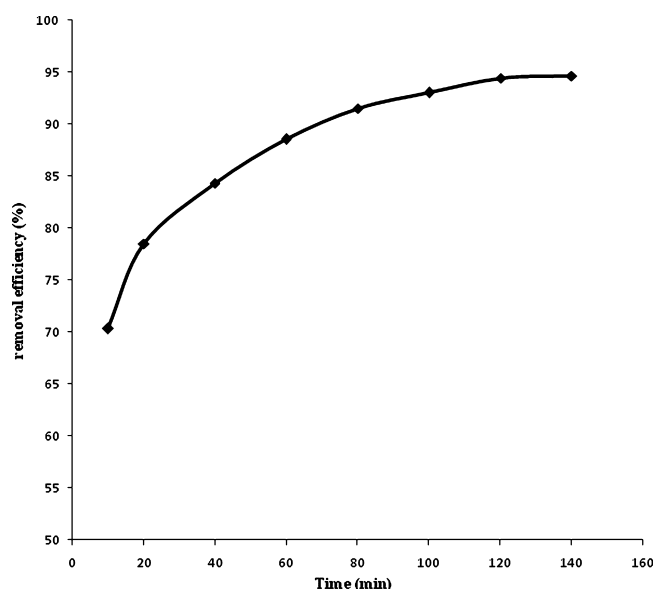


Figure 3. Effect of contact time on the removal efficiency (the initial concentration, pH, volume of solution, and amount of adsorbent were 100 mg/L, 4, 100 mL, and 3 g, respectively).

that the solution pH influences the chemical speciation of the metal ions as well as the ionization of the functional groups onto the adsorbent surfaces. In order to evaluate the influence of this parameter on the adsorption, the experiments were carried out at different initial pH values. The effect of pH on adsorption efficiencies are shown in Figure 5. The optimum pH value of 4 is observed for the Ni(II). The low degree of adsorption at low pH values can be explained by the fact that at low pH values the  $H^+$  ion concentration is high and therefore protons can compete with the lead cations for surface sites. In addition when pH increases, there is a decrease in positive surface charge (since the deprotonation of the sorbent functional groups could be occurs), which results in a lower electrostatic repulsion between the positively charged metal ion and the surface of ash, favoring adsorption.

**Kinetics of Sorption.** Most of the adsorption transformation processes of various solid phases are time dependent. To understand the dynamic interactions of Ni(II) with ash and

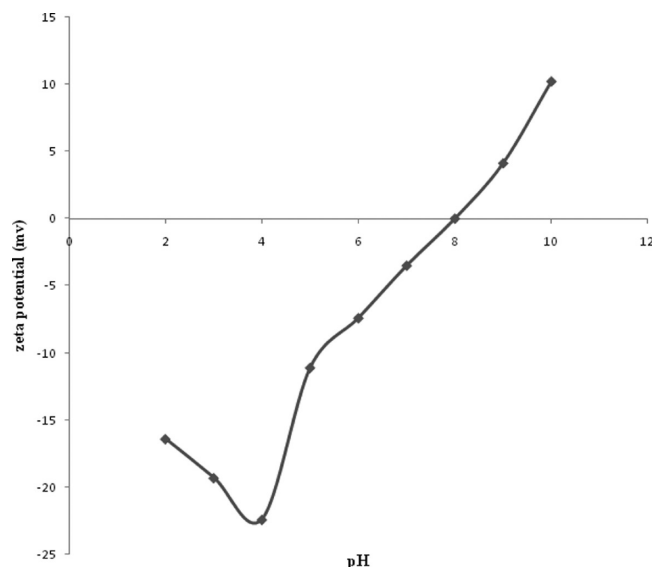


Figure 4. Zeta-potential of the ash at various pH's.

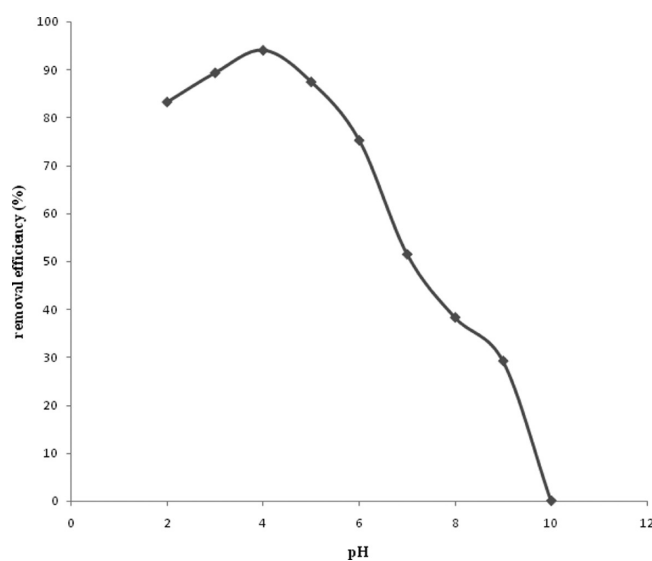


Figure 5. Effect of pH on the removal efficiency (the initial concentration, contact time, volume of solution, and amount of adsorbent were 100 mg/L, 120 min, 100 mL, and 3 g, respectively).

to predict their fate with time, knowledge of the kinetics of these processes is important.<sup>31</sup>

Although several models have been used for batch reactors to describe the transport of adsorbates inside adsorbent particles,<sup>32,33</sup> the mathematical complexity of these models makes them inconvenient for practical use. Simple and explicit relationships between the adsorption performance and operating conditions are therefore preferable. In this respect, lumped kinetic models, which how the spatially averaged solid phase concentration ( $q_t$ ) changes with adsorption time, are much simpler and easier to apply for practical operations. Models in this category include pseudofirst- and pseudosecond-order rate equations and the intraparticle diffusion model. The pseudofirst- and pseudo-second-order models assume that the difference between the average solid phase concentration ( $q_t$ ) and the equilibrium concentration ( $q_e$ ) is the driving force for adsorption and that the overall adsorption rate is proportional to this driving force. Both equations have been widely applied to explain the

experimental results obtained for aqueous pollutants such as dyes and metal ions.<sup>33–36</sup>

The adsorbate transport from the solution phase to the surface of the adsorbent particles occur in several steps. The overall adsorption process may be controlled either by one or more steps, e.g., film or external diffusion, pore diffusion, surface diffusion and the adsorption on the pore surface, or a combination of more than one steps. In a rapidly stirred batch adsorption, the diffusive mass transfer can be related by an apparent diffusion coefficient, which will fit the experimental sorption-rate data. Generally, a process is diffusion controlled if its rate dependent upon the rate at which components diffuse toward one another. To investigate the change in the concentration of sorbate onto sorbent with shaking time, the kinetic data of Ni(II) ions sorption onto ash were subjected to Morris–Weber (intraparticle) eq 4<sup>37</sup>

$$q_t = K_{id}(t^{0.5}) + C \quad (4)$$

where  $q_t$  is the sorbed concentration of Ni(II) ions at time  $t$ . The plot of  $q_t$  versus  $t^{1/2}$  is given in Figure 4. The value of rate constant of Morris-weber transport,  $K_{id}$ , calculated from the slope of the linear plot are shown in Figure 6. The rate constant

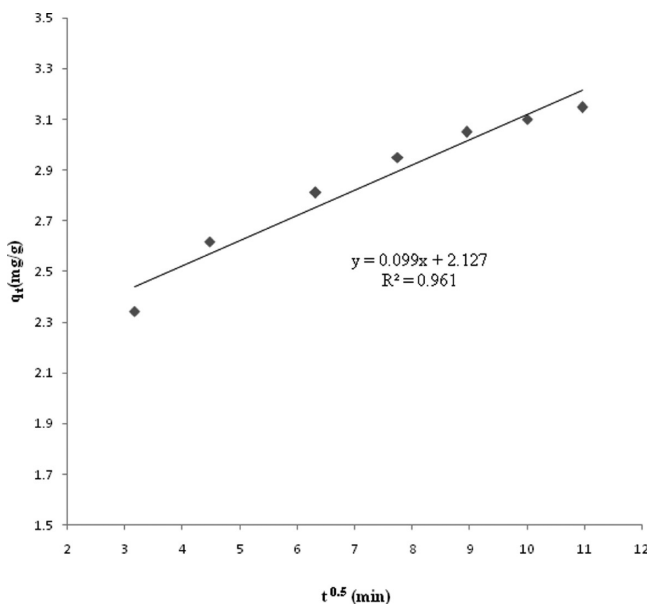


**Figure 6.** Morris–Weber plot of Ni(II) sorption onto ash (the initial concentration, pH, volume of solution, and amount of adsorbent were 100 mg/L, 4, 100 mL, and 3 g, respectively).

$k = 0.09 \text{ min}^{-1}$  was calculated from the slope of the straight line with a correlation factor of 0.961.

The pseudofirst order of the sorption of Ni(II) ions onto ash was evaluated by treating the data to the following form of Lagergren rate expression (5),<sup>38</sup> to determine the rate constant of sorption for Ni(II) ions–ash system:

$$\log(q_e - q_t) = \log q_e - (k/2.303)t \quad (5)$$

where  $q_e$  is the sorbed concentration at equilibrium and  $k$  is the first order rate constant. The linear plot of  $\log(q_e - q_t)$  against time  $t$  (Figure 7) demonstrates the applicability of the above equation for Ni (II) ions sorption onto ash. The rate constant  $k = 0.03 \text{ min}^{-1}$  was calculated from the slope of the straight line with a correlation factor of 0.95.

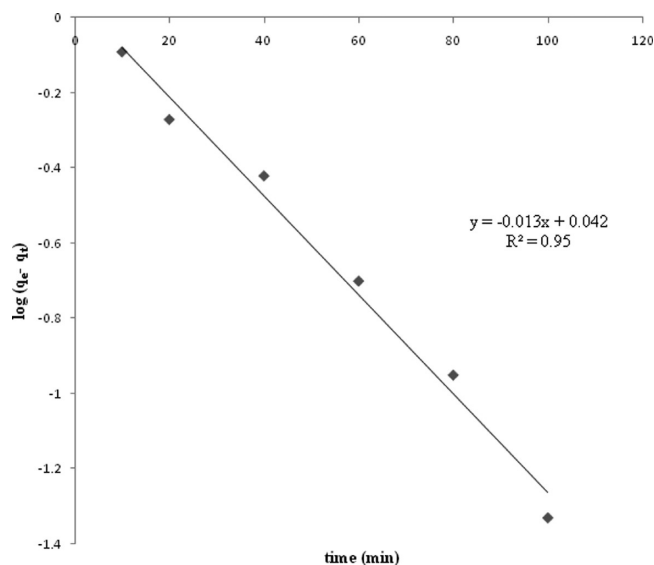


**Figure 7.** Validation of Lagergren plot of Ni(II) sorption onto ash (the initial concentration, pH, volume of solution, and amount of adsorbent were 100 mg/L, 4, 100 mL, and 3 g, respectively).

The kinetic data of Ni(II) ions sorption onto ash was subjected to pseudosecond order eq 6<sup>39</sup>

$$t/q_t = 1/(Kq_e^2) + t/q_e \quad (6)$$

The rate constant was calculated from the slope of the straight line (Figure 8). The rate constant was calculated from the slope

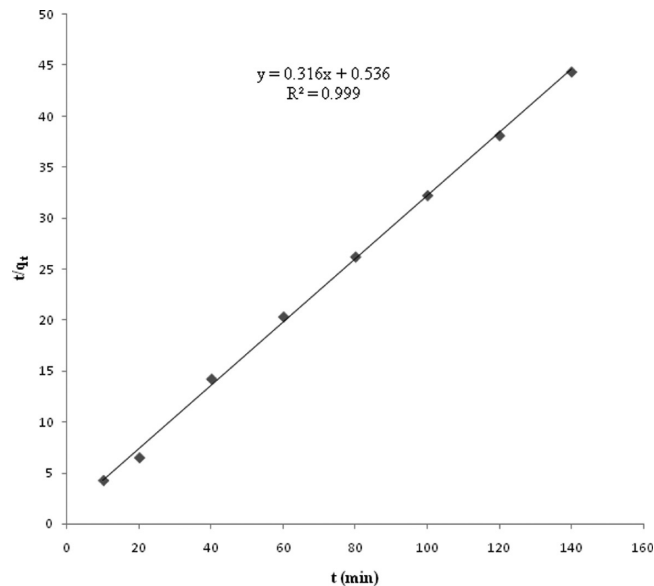


**Figure 8.** Pseudosecond order plot of Ni(II) sorption onto ash (the initial concentration, pH, volume of solution, and amount of adsorbent was 100 mg/L, 4, 100 mL, and 3 g, respectively).

of the straight line (Figure 8). The rate constant  $k = 0.24 \text{ min}^{-1}$  was calculated from the slope of the straight line with a correlation factor of 0.999. From Table 2, the kinetic data well fitted the pseudofirst-order, the pseudosecond-order and the intraparticle diffusion model. However, the correlation coefficients ( $r^2$ ) of pseudosecond-order are greater than pseudofirst-order which indicated that the pseudosecond order equation is

better than pseudofirst-order. So, the adsorption process was controlled by pseudosecond-order equation and the intraparticle diffusion model. The correlation coefficient of the intraparticle diffusion equation is lower than the pseudosecond-order equation. It could be interpreted as follows: first, the removal of Ni(II) from aqueous solution cannot be neglected relative to the amount of Ni(II) in the solution; second, the intraparticle diffusivity relies on the solid phase concentration in a large degree.<sup>40,41</sup> Due to the two reasons, the correlation coefficient of the intraparticle diffusion equation is not high. Also this suggests the assumption behind the pseudosecond-order model that the Ni(II) uptake process is due to chemisorptions.<sup>42</sup> The assumption behind the pseudosecond-order kinetic model was that the rate-limiting step might be chemisorptions involving valence forces through sharing or exchange of electrons between adsorbent and adsorbate.<sup>43,44</sup> Azizian<sup>45</sup> explored the kinetics of adsorption from a solution onto an adsorbent theoretically, and found that the adsorption process obeyed first-order kinetics at high initial concentration of solution while it obeyed pseudosecond-order kinetics at lower initial concentration of solution.

**Effect of Ash Dosage on Sorption of Ni(II).** Adsorbent dosage is an important parameter because this determines the capacity of an adsorbent for a given initial concentration of the adsorbate at the operating conditions. The effect of ash dose was studied for a by varying the dose between 0.5 and 4 g in 100 mL aqueous. These tests were conducted at a temperature of 20 °C, with optimum pH value for Ni(II). The initial metal ion concentration was 100 mg/L. It was observed that the adsorption percentage of Ni(II) onto the ash increased rapidly with the increasing of adsorbent concentration (Figure 9).

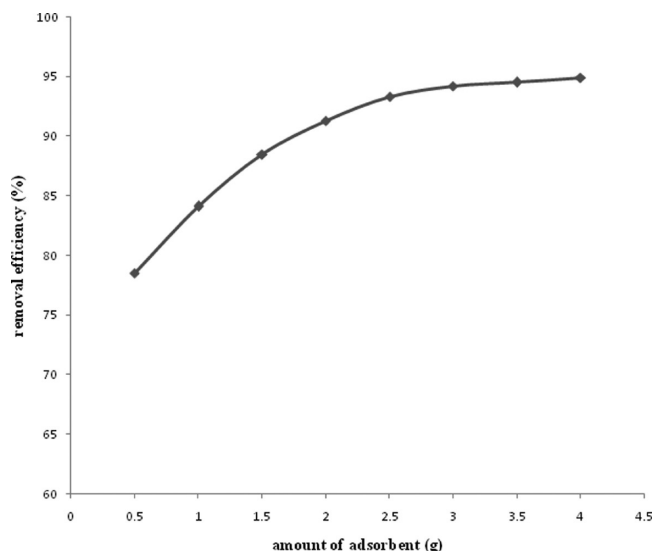


**Figure 9.** Effect of dosage on the removal efficiency (the initial concentration, pH, volume of solution, and contact time was 100 mg/L, 4, 100 mL, and 120 min, respectively).

This result is expected because the increase of adsorbent dose leads to greater surface area. When the adsorbent concentration was increased from 0.5 to 3 g, the percentage of Ni(II) ions adsorption increased from 76.3 to 94.2. At higher concentrations, the equilibrium uptake of Ni(II) did not increase significantly with increasing ash. Such behavior is expected due to the saturation level attained during an adsorption process.<sup>46</sup> For subsequent studies, a dose of 3 g of ash into 100 mL aqueous solution was selected. The data of Figure 9 were fitted to Langmuir,

Freundlich, and Dubnin–Randkovich (D-R) models in order to examine the models constants at different temperature adsorption isotherms.

**Isotherm Model.** The adsorption isotherm is based on the assumption that every adsorption site is equivalent and independent of whether or not adjacent sites are occupied. Isotherms show the relationship between metal concentration in solution and the amount of metal sorbed on a specific sorbent at a constant temperature.

**Langmuir Isotherm Model.** The Langmuir theory describes the monolayer coverage of adsorbate on a homogeneous adsorbent surface. The adsorption isotherm is based on the assumption that sorption takes place at specific homogeneous sites within the adsorbent and that once an adsorbate molecule occupies a site, no further adsorption can take place at that site. The saturation monolayer can be represented by the following expression (7):

$$q_e = (q_o K_L C_e) / (1 + K_L C_e) \quad (7)$$

where  $q_e$  is the amount of metal adsorbed per specific amount of adsorbent ( $\text{mg}\cdot\text{g}^{-1}$ ),  $C_e$  is equilibrium concentration of the solution ( $\text{mg}\cdot\text{L}^{-1}$ ), and  $q_o$  is the maximum amount of metal ions required to form a monolayer ( $\text{mg}\cdot\text{g}^{-1}$ ). The Langmuir equation can be rearranged to linear form for the convenience of plotting and determining the Langmuir constants ( $K_L$ ) as below. The values of  $q_o$  and  $K_L$  can be determined from the linear plot of  $C_e/q_e$  versus  $C_e$

$$\frac{C_e}{q_e} = \frac{1}{q_o K_L} + \frac{1}{q_o} C_e \quad (8)$$

The equilibrium data were analyzed using the linearized form the Langmuir adsorption isotherm eq 8. The Langmuir constants,  $K_L$ , and monolayer sorption capacity,  $q_o$ , were calculated from the slope and intercept of the plot between  $C_e/q_e$  and  $C_e$  (Figure 10). The results and equations are indicated in Figure 10

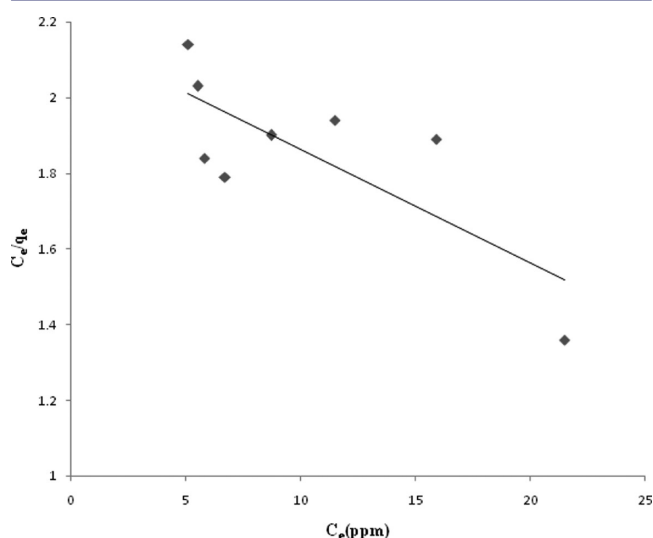


**Figure 10.** Langmuir sorption isotherm for Ni(II) (the initial concentration, pH, volume of solution, and contact time was 100 mg/L, 4, 100 mL, and 120 min, respectively).

and Table 4. As can be seen, the slope of line is negative, so this equation is not suitable for these data.

**Freundlich Isotherm Model.** While Langmuir isotherm assumes that enthalpy of adsorption is independent of the



Table 4. Isotherm Constant for Ni(II) Adsorption onto Ash

Langmuir equation		
$y = -0.0301x + 2.1718$		
Freundlich parameter		
$k$	$n$	$r$
0.363	0.84	0.98
D-R parameter		
$q_m$	$\beta$	$r^2$
10.86	$1 \times 10^{-6}$	0.88

amount adsorbed, the empirical Freundlich equation, based on sorption on heterogeneous surface, can be derived assuming a logarithmic decrease in the enthalpy of adsorption with the increase in the fraction of occupied sites. The Freundlich equation is purely empirical based on sorption on heterogeneous surface and is given by

$$q_e = K_F(C_e)^{1/n} \quad (9)$$

$K_F$  and  $(1/n)$  are the Freundlich constant and adsorption intensity, respectively. Equilibrium constants evaluated from the intercept and the slope, respectively, of the linear plot of  $\log q_e$  versus  $\log C_e$  based on experimental data. The Freundlich equation can be linearized in logarithmic form for the determination of the Freundlich constants as shown below

$$\log(q_e) = \log(K_F) + 1/n \log(C_e) \quad (10)$$

The slope and the intercept correspond to  $(1/n)$  and  $K_F$ , respectively. It was revealed that the plot of  $\log q_e$  and  $\log C_e$  yields a straight line (Figure 11). The results are indicated in Table 4.

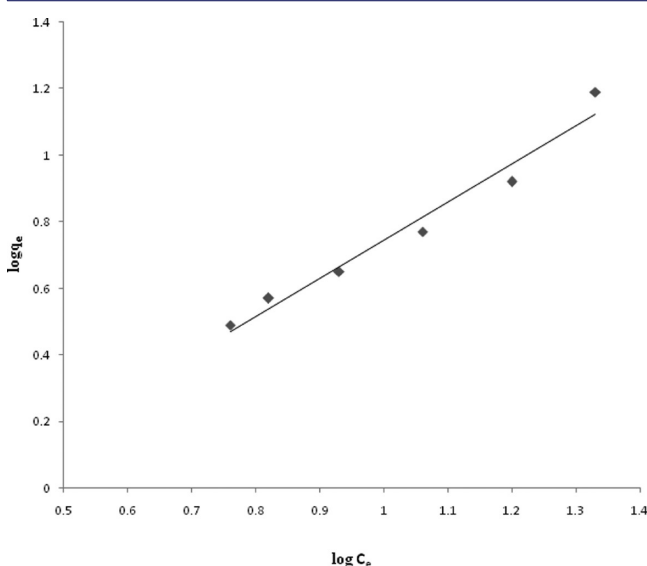


Figure 11. Freundlich sorption isotherm for Ni(II) (the initial concentration, pH, volume of solution, and contact time was 100 mg/L, 4, 100 mL, and 120 min, respectively).

The Freundlich isotherm constants  $K_F$  and  $n$  are constants incorporating all factors affecting the adsorption process such as of adsorption capacity and intensity of adsorption. The constants  $K_F$  and  $n$  were calculated from eq 10 using Freundlich plots as shown in Figure 11. The values for Freundlich constants and correlation coefficients ( $r^2$ ) for the adsorption process

are also presented in Table 4. The values of  $n$  between 1 and 10 (i.e.,  $1/n$  less than 1) represent a favorable adsorption. The values of  $n$ , which reflects the intensity of adsorption, also reflected the same trend. The  $n$  values obtained for the adsorption process represented a beneficial adsorption. The Freundlich-type adsorption isotherm is an indication of surface heterogeneity of the adsorbent while Langmuir-type isotherm hints toward surface homogeneity of the adsorbent. This leads to the conclusion that the surface of ash is made up of small heterogeneous adsorption patches which are very much similar to each other with respect to adsorption phenomenon.<sup>47,48</sup>

**D-R Isotherm Model.** The D-R<sup>49–51</sup> model was chosen to estimate the characteristic porosity and the apparent free energy of adsorption. The model assumed that the characteristics of the sorption curves are related to the porosity of the adsorbent. The linear form of this model is expressed by

$$\ln(q_e) = \ln(q_m) - \beta \epsilon^2 \quad (11)$$

where  $q_e$  is the amount of Ni(II) adsorbed per unit dosage of the adsorbent ( $\text{mg} \cdot \text{g}^{-1}$ ),  $q_m$  is the monolayer capacity (theoretical maximum capacity),  $\beta$  (model constant ( $\text{mol}^2 \cdot \text{KJ}^{-2}$ ) or the porosity factor) is the activity coefficient related to mean sorption energy, and  $\epsilon$  is the Polanyi potential described as

$$\epsilon = RT \ln[1 + (1/C_e)] \quad (12)$$

where  $R$  is a gas constant in  $\text{kJ} \cdot \text{mol}^{-1} \cdot \text{K}^{-1}$ ,  $T$  is the temperature in Kelvin, and  $C_e$  is as defined earlier. From the plots of  $\ln q_e$  versus  $\epsilon^2$  (Figure 12) the values of  $\beta$  and  $q_m$  were determined by the

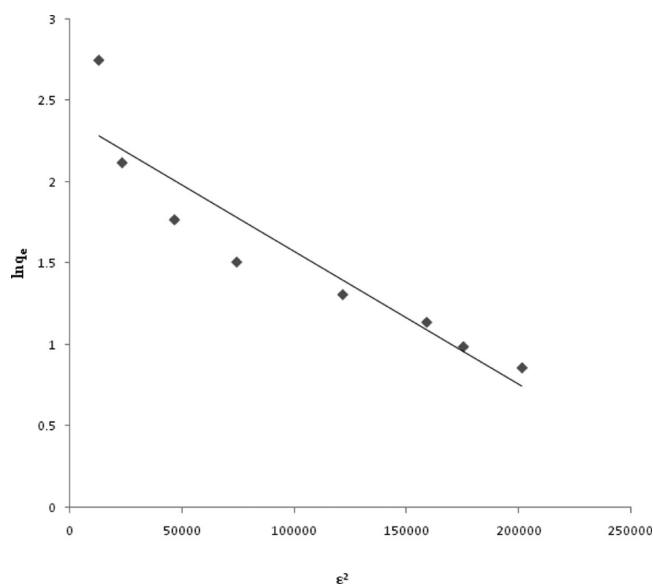


Figure 12. D-R sorption isotherm for Ni(II) (the initial concentration, pH, volume of solution, and contact time was 100 mg/L, 4, 100 mL, and 120 min, respectively).

slope and intercept of the linear plot. The value of  $E$  evaluated from the slope ( $\beta$ ) of D-R curve using equation ( $E = 1/\sqrt{2\beta}$ ) is  $11.8 \text{ kJ} \cdot \text{mol}^{-1}$  which is in the range of  $9\text{--}16 \text{ kJ} \cdot \text{mol}^{-1}$ , expected for chemisorptions or ion exchange. The statistical results along with the isotherm constants are also given in Table 1. As our results show, adsorption of Ni(II) by ash can be fitted using Freundlich equation also the D-R equation shows considerable correlation factor. Although the Freundlich isotherm provides the information



about the surface heterogeneity and the exponential distribution of the active sites and their energies, it does not predict any saturation of the surface of the adsorbent by the adsorbate. Hence, infinite surface coverage could be predicted mathematically. In contrast, D-R isotherm relates the heterogeneity of energies close to the adsorbent surface. If a very small subregion of the sorption surface is chosen and assumed to be approximately by the Langmuir isotherm, the quantity can be related to the mean sorption energy,  $E$ , which is the free energy for the transfer of 1 mol of metal ions from the infinity to the surface of the adsorbent.<sup>40,41</sup>

**Effect of Initial Concentration of Ni(II) on the Adsorption.** The experiments were carried out using various concentrations of Ni(II) solution under the determined optimum pH values and contact time. The effect of initial Ni(II) ion concentration was investigated in the range of 100–1000 mg·L<sup>-1</sup>. The results are presented in Figure 13. The Ni(II)

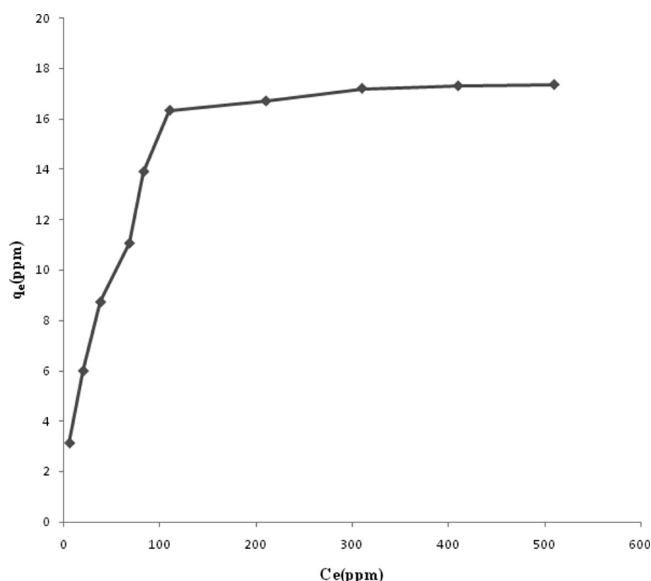


**Figure 13.** Effect of initial concentration on the removal efficiency (the amount of ash, pH, volume of solution, and contact time was 3, 4, 100 mL, and 120 min, respectively).

adsorption capacity of the ash first increased with increasing the initial concentration of metal ion and then reached a saturation value at about 600 mg·L<sup>-1</sup> and the maximum equilibrium uptake for Ni(II) was 16.3 mg·g<sup>-1</sup>. Then the value did not significantly change with the initial metal ion concentration. The results indicate that there is a reduction in Ni(II) adsorption, owing to the lack of available active sites required for the high initial concentration of Ni(II). The higher uptake of Ni(II) at low concentration may be attributed to the availability of more active sites on the surface of the adsorbent for lesser number of adsorbate species.

## ■ ADSORPTION THERMODYNAMICS

**Effect of Temperature on Adsorption of Ni(II).** To study the effect of temperature adsorption experiments are carried out at 20–50 °C at optimum pH value of materials and adsorbent dosage level of 3 g in 100 mL of solutions. The equilibrium contact time for adsorption was maintained at 2 h. The percentage of adsorption increases with rise of temperature from 20 to 50 °C. The results were shown in Table 5 and it revealed the endothermic nature of the adsorption process

**Table 5.** Effect of Temperature on the Removal Efficiency

temperature, °C	removal efficiency of Ni
20	94.2
30	95.1
40	96.7
50	97.5

which later utilized for determination of changes in Gibbs free energy ( $\Delta G$ ), heat of adsorption ( $\Delta H$ ), and entropy ( $\Delta S$ ) of the adsorption of Ni(II) from aqueous solutions. The increase in adsorption with rise in temperature may be due to the strengthening of adsorptive forces between the active sites of the adsorbents and adsorbate species and between the adjacent molecules of the adsorbed phase.

**Effect of Temperature on Thermodynamics Parameter on Adsorption of Ni(II).** To study the thermodynamics of adsorption of Ni(II) on ash, thermodynamic constants such as enthalpy change  $\Delta H$ , free energy change  $\Delta G$  and entropy change  $\Delta S$  were calculated using eqs 13–15. The values of these parameters are given in Table 6. Thermodynamic parameter  $\Delta H$ ,

**Table 6.** Thermodynamic Parameter for Adsorption of Ni(II) onto Ash

	$\Delta H$ (kJ·mol <sup>-1</sup> )	$\Delta S$ (kJ·kmo <sup>-1</sup> )	$T$ (°C)	$\Delta G$ (kJ·mo <sup>-1</sup> )	$r^2$
Ni	23.83	0.1	20	-48.7	0.98
			30	-75.5	
			40	-104.1	
			50	-134.7	

$\Delta S$ , and  $\Delta G$  for the Ni(II) ions–ash system were calculated using the following equations:

$$K_c = F_e / (1 - F_e) \quad (13)$$

$$\log K_c = - \Delta H / (2.303RT) + \Delta S / (2.303R) \quad (14)$$

$$\Delta G = - RT \ln K_c \quad (15)$$

where  $F_e$  is the fraction of Ni(II) ions sorbed at equilibrium. It is noted that all  $\Delta G$  values shown in Table 6 are negative. This suggests that the adsorption process is spontaneous with high preference of Ni(II) for ash. The free energy (negative values) increases (from -48.7 to -134.7 kJ/mol) with an increase of temperature from 20–50 °C, which clearly shows that the process is favorable at higher temperature. The changes of energy for physical adsorption are generally smaller than that of chemisorption. The changes of energy for physical adsorption are in the range of 0 to 19.646 kJ·mol<sup>-1</sup>, and that of chemical adsorption -59.42 to -397.1 kJ·mol<sup>-1</sup>.<sup>52</sup> As shown in Table 3, the magnitude of adsorption free energy ( $\Delta G$ ) ranging from -48.7 to -134.7 kJ·mol<sup>-1</sup> suggests that the adsorption can be considered as a chemisorption. The enthalpy change  $\Delta H$  is positive (endothermic) due to increase in adsorption on successive increase in temperature. The positive value of  $\Delta S$  reveals the increased randomness at the solid–solution interface during the fixation of the ion on the active sites of the sorbent. The positive value of  $\Delta S$  suggests the increased randomness at the solid–solution interface during the adsorption of Ni (II) ions on ash. On the adsorption of Ni (II), the adsorbed solvent molecules, which are displaced by the adsorbate species, gain more translational entropy than is lost

by the adsorbate ions, thus allowing for the prevalence of randomness in the system.<sup>53</sup>

**Desorption Experiments.** To check whether metal ion can be desorbed from the exhaust ash, two tests were carried out to simulate the leaching as well by rainwater (test by water saturated with carbon dioxide) as by NaOH percolates. Table 7

**Table 7. Desorption Efficiency Test by CO<sub>2</sub> or NaOH Aqueous Solution**

element	NaOH concentration (M)	desorption using NaOH (%)	desorption using CO <sub>2</sub> (%)
Ni	0.1	7.12	25.5
	0.2	14.83	
	0.3	23.32	
	0.4	26.71	
	0.5	31.42	
	0.6	31.76	
	0.7	32.25	

reports that the desorption efficiency is not considerable. As can be seen, NaOH concentration increase has positive effect on the desorption process but after 0.5 M, the NaOH concentration has not significant effect on the desorption efficiency. Findings indicate the low reversibility of the sorption process at the pH values of both tests. Leaching by NaOH is more effective than by CO<sub>2</sub>-saturated water.

**Application of Ash for Removal of the Heavy Metals and COD from Plating Wastewater.** Upon completion of basic adsorption experiments, the efficacy of ash in the removal of Cr(VI), Zn(II), Ni, and COD from industrial wastewater was evaluated. To this end, a bulk wastewater sample was obtained from a local plating wastewater (Shahi, Iran). The pH, color, and material concentration of collected wastewater was determined at the beginning of adsorption experiments, are shown in Table 8. The pH of wastewater was 3.4. Adsorption

**Table 8. Characteristics of Plating Wastewater and Removal Efficiency after Treatment by Ash**

compound	concentration in wastewater	removal efficiency of ash (%)
COD (mg/L)	143	68.3
Cr (mg/L)	328	75.4
Ni (mg/L)	32.5	91.5
Zn (mg/L)	15.2	92.8
color (absorbance at 600 nm)	0.35	63.5

was performed on 100 mL of wastewater with an ash dose of 3 g. The suspensions were stirred at room temperature (20 °C) and 200 rpm. Table 8 shows Cr(VI), Zn(II), Ni, and COD removal from wastewater in terms of percent removal. As can be seen, ash is an efficient and cost-effective adsorbent for the removal of Cr(VI), Zn(II), Ni, and COD from industrial wastewaters. The main advantages of ash for the removal of Cr(VI), Zn(II), Ni, and COD from water and wastewater include a high adsorption rate, capacity, and efficacy, as well as a short equilibration time. Furthermore, ash is available as a no-cost waste and can be used without modifications. Thus, ash adsorption is environmentally friendly and achieves treatment goals in a simple and low-cost manner.

## CONCLUSIONS

Adsorption studies on ash have been shown to be highly effective in removing of Ni(II) from aqueous solution. This adsorbent is widely available as a waste material, is mechanically stable, and most importantly is environmentally appealing. In addition, this adsorbent does not mix with water, and it can be separated very easily from water. The maximum Ni(II) ions adsorption capacity of ash is very close to other adsorbents. Therefore, it may be used as an alternative adsorbent, replacing costly materials, such as activated carbon, resins, etc. The maximum Ni(II) ions is 94.2 %. The optimum conditions of sorption were found to be: a sorbent dose of 3 g in 100 mL of Ni(II) contact time of 120 min, pH 4 for the Ni(II). The results gained from this study were well described by the theoretical Freundlich. The kinetic data indicated that the adsorption process was controlled by pseudosecond-order equation. Desorption of Ni(II) from ash have been studied using 0.5 M NaOH and by water saturated with CO<sub>2</sub>, maximum desorption efficiency was 35%. The effect of temperature has been studied; it was found that increasing temperature has positive effect on the adsorption, the thermodynamic parameters  $\Delta H$ ,  $\Delta S$ , and  $\Delta G$  are evaluated. Thermodynamic parameters showed that the adsorption of Ni(II) onto ash was feasible, spontaneous and endothermic under studied conditions also ash was used in plating wastewater treatment that the results is considerable.

## AUTHOR INFORMATION

### Corresponding Author

\*E-mail: Mazyar.Sharifzadeh@gmail.com. Fax: +982182883381.

### Funding

This research was supported by a grant from Pars Gas & Oil Co. and Islamic Azad University.

## ACKNOWLEDGMENTS

Hooman Taher Rahmati at Tarbiat Modares University is acknowledged for his assistance with experimental design and analysis.

## REFERENCES

- (1) Boudrahem, F.; Soualah, A.; Aissani-Benissad, F. Pb(II) and Cd(II) Removal from Aqueous Solutions Using Activated Carbon Developed from Coffee Residue Activated with Phosphoric Acid and Zinc Chloride. *J. Chem. Eng. Data* **2011**, *56* (5), 1946–1955.
- (2) Sharma, Y. C.; Srivastava, V. Comparative Studies of Removal of Cr(VI) and Ni(II) from Aqueous Solutions by Magnetic Nanoparticles. *J. Chem. Eng. Data* **2011**, *56* (4), 819–825.
- (3) Kadirvelu, K.; Thamaraiselvi, K.; Namasivayam, C. Adsorption of nickel(II) from aqueous solution onto activated carbon prepared from coirpith. *Sep. Purif. Technol.* **2001**, *24*, 497–505.
- (4) Danish, M.; Hashim, R.; Ibrahim, M. N. M.; Rafatullah, M.; Sulaiman, O.; Ahmad, T.; Shamsuzzoha, M.; Ahmad, A.; Sorption of Copper(II) and Nickel(II) Ions from Aqueous Solutions Using Calcium Oxide Activated Date (Phoenix dactylifera) Stone Carbon: Equilibrium, Kinetic, and Thermodynamic Studies, *J. Chem. Eng. Data*, **2011**, DOI: 10.1021/jc200460n
- (5) Babel, S.; Kurniawan, T. A. Low-cost adsorbents for heavy metals uptake from contaminated water: a review. *J. Hazard. Mater.* **2003**, *97*, 219–243.
- (6) Kadirvelu, K.; Namasivayam, C. Activated carbon from coconut coir pith as metal adsorbent: adsorption of Cd(II) from aqueous solution. *Adv. Environ. Res.* **2003**, *7*, 471–478.
- (7) Wilson, A. R.; Lion, L. W.; Nelson, Y. M. Pb scavenging from a freshwater lake by Mn oxides in heterogeneous surface coating materials. *Environ. Sci. Technol.* **2001**, *35*, 3182–3189.

- (8) Pan, S. C.; Lin, C. C.; Tseng, D. H. Reusing sewage sludge ash as adsorbent for copper removal from wastewater. *Resour. Conserv. Recycl.* **2003**, *39*, 79–90.
- (9) Low, K. S.; Lee, C. K.; Leo, A. C. Removal of metals from electroplating wastes using banana pith. *Bioresour. Technol.* **1995**, *51*, 227–231.
- (10) Sarioglu, M.; Atay, Ü. A.; Cebeci, Y. Removal of copper from aqueous solutions by phosphate rock. *Desalination* **2005**, *181*, 303–311.
- (11) Malandrino, M.; Abollino, O.; Giacomino, A.; Aceto, M.; Mentasti, E. Adsorption of heavy metals on vermiculite: influence of pH and organic ligands. *J. Colloid Interface Sci.* **2006**, *299*, 537–546.
- (12) Boonfueng, T.; Axe, L.; Xu, Y.; Tyson, T. A. Nickel and lead sequestration in manganese oxide-coated montmorillonite. *J. Colloid Interface Sci.* **2006**, *303*, 87–98.
- (13) Gupta, V. K.; Saini, V. K.; Jain, N. Adsorption of As(III) from aqueous solutions by iron oxide-coated sand. *J. Colloid Interface Sci.* **2005**, *288* (1), 55–60.
- (14) Boujelben, N.; Bouzid, J.; Elouear, Z.; Feki, M.; Jamoussi, F.; Montiel, A. Phosphorus removal from aqueous solution using iron coated natural and engineer adsorbents. *J. Hazard. Mater.* **2008**, *151* (1), 103–110.
- (15) Han, R. H.; Zou, W.; Zhang, Z. P.; Shi, J.; Yang, J. J. Removal of copper(II) and lead(II) from aqueous solution by manganese oxide coated sand: I. Characterization and kinetic study. *J. Hazard. Mater.* **2006**, *137* (1), 384–395.
- (16) Han, R. H.; Zou, W.; Li, H.; Li, Y.; Shi, J. Copper(II) and lead(II) removal from aqueous solution in fixed-bed columns by manganese oxide coated zeolite. *J. Hazard. Mater.* **2006**, *137* (2), 934–942.
- (17) Han, R. H.; Zou, W.; Zhang, Z. P.; Shi, J.; Yang, J. J. Kinetic study of adsorption of Cu(II) and Pb(II) from aqueous solutions using manganese oxide coated zeolite in batch mode. *Colloid Surf. A: Phys. Eng. Asp.* **2006**, *279* (1–3), 238–246.
- (18) Khraisheh, M.; Al-degs, S.; Wendy, A. M. M. Remediation of wastewater containing heavy metals using raw and modified diatomite. *Chem. Eng. J.* **2004**, *99* (2), 177–184.
- (19) Manz, O. E. Coal fly ash: a retrospective and future look. *Fuel* **1999**, *78*, 133–136.
- (20) Toscano, G.; Caristi, C.; Cimino, G. Sorption of heavy metal from aqueous solution by volcanic ash. *C. R. Chimie* **2008**, *11*, 765–771.
- (21) Xenidis, A.; Mylona, E.; Pospaliaris, I. Potential use of lignite fly ash for the control of acid generation from sulphidic wastes. *Waste Manage.* **2002**, *22*, 631–41.
- (22) Rio, S.; Delebarre, A. Removal of mercury in aqueous solution by fluidized bed plant fly ash. *Fuel* **2003**, *82*, 153–9.
- (23) Viraraghavan, T.; Dronamraju, M. M. Utilization of coal ash in water pollution control. *Int. J. Environ. Stud.* **1992**, *40*, 79–85.
- (24) Gupta, V. K.; Sharma, S.; Yadav, I. S.; Mohan, D. Utilization of bagasse fly ash generated in the sugar industry for the removal and recovery of phenol and p-nitrophenol from wastewaters. *Technol. Biotechnol.* **1998**, *71*, 180–6.
- (25) Janos, P.; Buchtov, H.; Ryznarova, M. Sorption of dyes from aqueous solutions onto fly ash. *Water Res.* **2003**, *37*, 4938–4944.
- (26) Gupta, V. K.; Mohan, D.; Sharma, S.; Sharma, M. Removal of basic dye (Rhodamine B and Methylene Blue) from aqueous solutions using bagasse fly ash. *Sep. Sci. Technol.* **2000**, *35*, 2097–2113.
- (27) Mohan, D.; Singh, K. P.; Singh, G.; Kumar, K. Removal of dyes from wastewater using fly ash, a low-cost adsorbent. *Ind. Eng. Chem. Res.* **2002**, *41*, 3688–3695.
- (28) Brunori, C.; Balzamo, S.; Morabito, R. Comparison between different leaching tests for the evaluation of metal release from fly ash. *Fresenius. J. Anal. Chem.* **2001**, *371*, 843–8.
- (29) Srivastava, V. C.; Mall, I. D.; Mishra, I. M. Characterization of mesoporous rice husk ash (RHA) and adsorption kinetics of metal ions from aqueous solution onto RHA. *J. Hazard. Mater.* **2006**, *134*, 257–267.
- (30) Lee, K. M. Interface Properties of Nickel-silicide Films Deposited by Using Plasma-assisted Atomic Layer Deposition. *J. Korean Phys. Soc.* **2009**, *55* (3), 1153–1157.
- (31) Karakus, M.; Alpoguz, H. K.; Kaya, A.; Acar, N.; Gorgulu, A. O.; Arslan, M. A kinetic study of mercury(II) transport through a membrane assisted by new transport reagent. *Chem. Cent. J.* **2011**, *5*, 43–49.
- (32) Do, D. D. *Adsorption Analysis: Equilibria and Kinetics*; Imperial College Press: London, 1998.
- (33) Ho, Y. S.; McKay, G. Pseudo-second order model for sorption processes. *Process Biochem.* **1999**, *34*, 451–465.
- (34) Ho, Y. S.; McKay, G. Sorption of dyes and copper ions onto biosorbents. *Process Biochem.* **2003**, *38*, 1047–1061.
- (35) Liu, Y.; Shen, L. From Langmuir kinetics to first- and second-order rate equations for adsorption. *Langmuir* **2008**, *24*, 11625–11630.
- (36) Azizian, S.; Haerifar, M.; Bashiri, H. Adsorption of methyl violet onto granular activated carbon: equilibrium, kinetics and modeling. *Chem. Eng. J.* **2009**, *146*, 36–41.
- (37) Morris, W. J.; Weber, C. I. Kinetics of adsorption on carbon from solution. *J. Saint. Eng. Div., ASCE.* **1963**, *89*, 31–62.
- (38) Lagergren, S. Z. *Sogeuanten Adsorption Gelosterstoffe Handlingar* **1898**, *24*.
- (39) Bhattacharya, A. K.; Naiya, T. K.; Mandal, S. N.; Das, S. K. Adsorption, kinetics and equilibrium studies on removal of Cr(VI) from aqueous solutions using different low-cost adsorbents. *Chem. Eng. J.* **2008**, *137*, 529–541.
- (40) Yang, X. Y.; Otto, S. R.; Bushra, A. D. Concentration-dependent surface diffusivity model (CDSDM): numerical development and application. *J. Chem. Eng.* **2003**, *94*, 199–209.
- (41) Yang, X. Y.; Bushra, A. D. Application of branched pore diffusion model in the adsorption of reactive dyes on activated carbon. *J. Chem. Eng.* **2001**, *83*, 15–23.
- (42) Seleem, H. S.; El-Inany, G. A.; El-Shetary, B. A.; Mousa, M. A.; Hanafy, F. I. The ligational behavior of an isatinic quinolyl hydrazone towards copper(II)-ions. *Chem. Cent. J.* **2011**, *5*, 20–29.
- (43) Ho, Y. S.; McKay, G. The kinetics of sorption of divalent metal ions onto sphagnum moss peat. *Water Res.* **2000**, *34* (30), 735–742.
- (44) Calero, M.; Blazquez, G.; MartiLara, M. A. Kinetic Modeling of the Biosorption of Lead(II) from Aqueous Solutions by Solid Waste Resulting from the Olive Oil Production. *J. Chem. Eng. Data* **2011**, *56* (7), 3053–3060.
- (45) Azizian, S. Kinetic models of sorption: a theoretical analysis. *J. Colloid Interface Sci.* **2004**, *276*, 47–52.
- (46) Mahramanlioglu, M.; Kizilcikli, I.; Bicer, I. O. Adsorption of fluoride from aqueous solution by acid treated spent bleaching earth. *J. Fluorine Chem.* **2002**, *115*, 41–47.
- (47) Katal, R.; pahlavanzadeh, H. Zn(II) ion removal from aqueous solution by using a polyaniline composite. *J. Vinyl Addit. Technol.* **2011**, *17* (2), 138–145.
- (48) Basha, S.; Jha, B. Estimation of Isotherm Parameters for Biosorption of Cd(II) and Pb(II) onto Brown Seaweed, *Lobophora variegata*. *J. Chem. Eng. Data* **2008**, *53* (2), 449–455.
- (49) Dubinin, M. M.; Radushkevich, L. V. Equation of the characteristic curve of activated charcoal. *Proc. Acad. Sci. U.S.S.R. Phys. Chem. Sect.* **1947**, *55*, 331.
- (50) Omraei, M.; Esfandian, H.; Katal, R.; Ghorbani, M. Study of the removal of Zn(II) from aqueous solution using polypyrrole nano-composite. *Desalination* **2011**, *271*, 248–256.
- (51) Katal, R.; Ghiass, M.; Esfandian, H. Application of Nanometer Size of Polypyrrole as a Suitable Adsorbent for Removal of Cr(VI). *J. Vinyl Addit. Technol.* **2011**, *17* (3), 222–230.
- (52) Jaycock, M. J.; Parfitt, G. D. *Chemistry of interfaces*; Ellis Horwood Limited: New York, 1981.
- (53) Gupta, V. K.; Jain, R.; Siddiqui, M. N.; Saleh, T. A.; Agarwal, S.; Malati, S.; Pathak, D. Equilibrium and Thermodynamic Studies on the Adsorption of the Dye Rhodamine-B onto Mustard Cake and Activated Carbon. *J. Chem. Eng. Data* **2010**, *55* (11), 5225–5229.